Proceedings of the ASME 2017 36th International Conference on Ocean, Offshore and Arctic Engineering
OMAE2017
June 25-30, 2017, Trondheim, Norway

OMAE2017-62034

A NUMERICAL STUDY ON A FLOPPER STOPPER FOR LEG POSITIONING OF A JACK-UP BARGE

Zhiyu Jiang
Centre for Research-based Innovation
on Marine Operations (*SFI MOVE*),
Department of Marine Technology,
Norwegian University of Science and Technology
NO-7491 Trondheim, Norway
Email: zhiyu.jiang@ntnu.no

Wilson Guachamin Acero
Department of Marine Technology,
Norwegian University of Science and Technology
NO-7491 Trondheim, Norway
Email: wilson.i.g.acero@ntnu.no

Zhen Gao
Centre for Research-based Innovation
on Marine Operations (*SFI MOVE*),
Centre for Autonomous Marine Operations and Systems (*AMOS*),
Department of Marine Technology,
Norwegian University of Science and Technology
NO-7491 Trondheim, Norway
Email: zhen.gao@ntnu.no

Lin Li
Department of Mechanical and Structural
Engineering and Materials Science,
University of Stavanger
NO-4036, Stavanger, Norway
Email: lin.li@uis.no

ABSTRACT

Jack-up barges are commonly used for marine operations in the offshore oil and gas, and offshore wind industries. A critical phase within the marine operation activities is the positioning of the jack-up legs onto the seabed. During this process, large impact velocities and forces may arise from the barge's heave, roll and pitch motions, and structural damage of the legs can occur. This paper numerically investigates the effect of a flopper stopper (FS) on the motion responses of a jack-up barge from the offshore wind industry. The FS is known as a passive roll compensation device. It is suspended from the side of the barge by means of wire ropes and cantilever beams. A simple geometry of an FS is proposed, and the working principle introduced. For the loading condition before the leg-soil impact occurs, global dynamic analyses of the coupled system are conducted. Characteristic values of impact velocities are used to establish the jack-up operational limits in terms of the significant wave height and peak period. By comparing the operational limits for the barge with and without FS, it is found that FS should be placed on the weather side. At beam seas, the current FS can lead to a maximum increase in the operational wave height limit of 35%, whereas for the other wave headings, it may not be beneficial to use FS.

INTRODUCTION

The number of offshore wind farms has been growing steadily over the years. Jack-up barges can provide a stable lifting platform for crane operations, and are normally used for installation and major components repair of offshore wind turbine components. Compared with purpose-built installation vessels with large capacities, self-propelled or propulsion-assisted vessels modified for servicing offshore wind

Copyright © 2017 ASME

Downloaded From: http://proceedings.asmedigitalcollection.asme.org/ on 09/28/2017 Terms of Use: http://www.asme.org/about-asme/terms-of-use

turbines can be more economically viable for operation and maintenance purposes [2].

When a jack-up platform is moving onto a location, there is a phase during which the legs touch the seabed and undergo impact loads. To avoid structural damage, the maximum impact forces that occur must be within allowable limits. These forces depend on impact mass, impact velocity, and soil mechanical properties. The impact force is not a practical parameter for onboard decision making. Instead, other environmental parameters or measurable vessel responses are desired [3]. A significant wave height (H_s) of 1.5 meters is a practical value used by the industry [4], although the origin of such limits is not clear. The H_s limit is not sufficient for floating structures, and the wave spectrum peak period (T_p) needs to be considered. Guachamin Acero et al. [5] proposed a methodology to establish the operational limits of marine operations in terms of allowable limits of sea states. These operational limits provide the same safety levels as a response parameter such as leg impact force or impact velocity. To increase the operational limits, the motions of jack-up barges, and thus the impact velocities need to be reduced. We may consider passive roll compensation systems for such purposes.

There exist various anti-roll devices. Among them, FS's are passive devices that have been widely applied to small vessels. Fig. 1 shows an application on a sailboat. McCreight et al. [6] showed the effectiveness of FS for a Torpedo Weapons Retriever at zero speed in random beam seas. Using a one degree-of-freedom (DOF) model for the system, the authors did analyses in the frequency domain. Bass [7] performed simulations and full-scale tests for fishing vessels using FS. It was noted that the vessel roll amplitudes for the leeward deployment were much higher than those for the weather-side depolyment of a single FS. This aspect was not considered by the simplified approach in [6]. To the authors' knowledge, FS devices have not been applied to jack-up barges and a detailed assessment of their applicability has not been published. In this paper, a preliminary assessment is made of the effectiveness of an FS. This is done by performing time-domain simulations and by comparing the allowable limits of sea states of the barge with and without the FS.

FIGURE 1. A flopper stopper suspended from a boom [1]

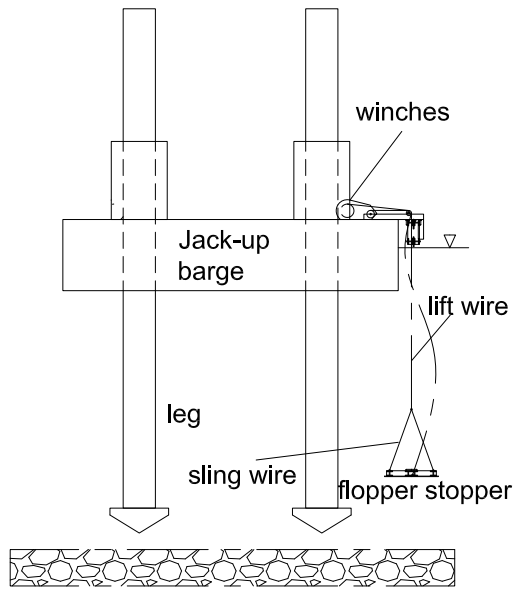

FIGURE 2. Schematic of a jack-up barge with a flopper stopper at work

DESCRIPTION OF THE FLOPPER STOPPER

Basic Design

Fig. 2 shows a jack-up barge with an FS at work when the legs of the barge are being lowered. The FS is suspended from the cantilever beam using wires. If FS and crane are on the same side, FS can be positioned closer to the vessel bow, and crane closer to the vessel stern.

A possible construction of the FS is in illustrated by Fig. 3. The FS is foldable and can be retrieved, see Fig. 3(a). A foldable FS allows its transportation on the side of a barge and reduces the wave load effects during the lowering process. In working conditions, the FS is open, see Fig. 3(b). The structure consists of bottom plates and stopper beams. The lifting padeyes are connected to the sling wires.

Working Principle

Heave motion of the FS is dominant and is coupled to the vessel roll and heave. Sway motion of the FS follows that of the vessel. Far below the free surface ($z_{FS} \leq$ -10 m), the FS is less affected by wave excitations, and experiences slight rotational motions.

Because of the sharp edges, the FS is subjected to large viscous forces during vertical motion. The forces on the FS

Copyright © 2017 ASME

Downloaded From: http://proceedings.asmedigitalcollection.asme.org/ on 09/28/2017 Terms of Use: http://www.asme.org/about-asme/terms-of-use

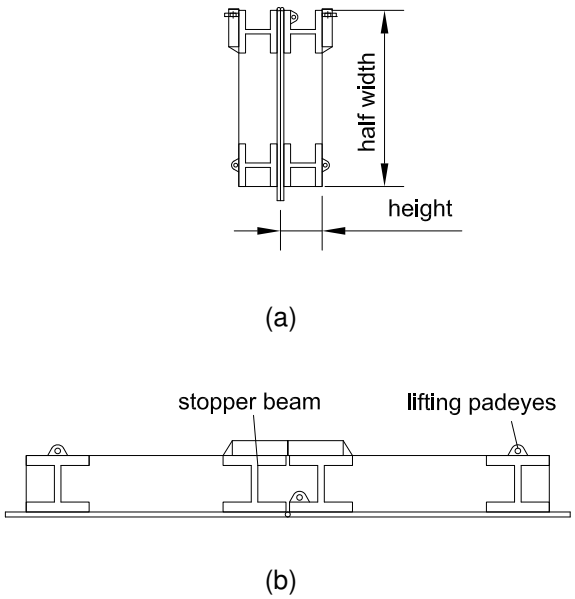

FIGURE 3. Schematic of a flopper stopper for jack-up barges (a) side view (folded) (b) front view (opened)

create a time-varying moment on the barge. Heave motion of the FS and roll motion of the barge are not entirely simultaneous. Thus, this moment can dissipate energy from, or input energy to the barge.

To estimate the dissiplated energy of an ideal FS during one cycle, we follow a simplified approach [6]. The vessel roll motion is assumed to be uncoupled from other motions, and the uncoupled linear roll equation in regular waves can be written as [8]

$$(I_{44}+A_{44})\ddot{\phi}(t)+B_{44}\dot{\phi}(t)+C_{44}\phi(t)=F_{\phi}(t) \tag{1}$$

where ϕ is the roll angle, I_{44} is the moment of inertia in roll, A_{44} is the roll added moment, B_{44} is the linear damping coefficient, C_{44} is the hydrostatic restoring moment, and F_{ϕ} is the roll exciting moment. When an FS is present, B_{44} alternates cyclically. Near the roll resonance, the importance of damping on the response should be emphasized, since the inertial and the hydrostatic restoring forces cancel each other and the net contribution is small.

Suppose the vessel roll motion is sinusoidal with amplitude ϕ_a, and the FS heave motion is in phase, then the vertical displacement can be expressed as

$$z_{FS}(t)=\eta_s sin(\omega t) \tag{2}$$

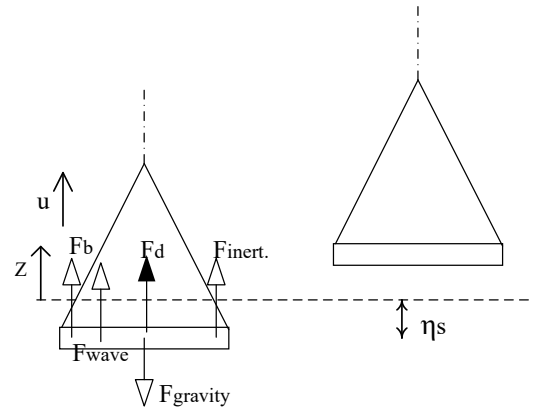

FIGURE 4. Positions of a flopper stopper during one half cycle

where η_s is the heave amplitude of the FS, ω is the circular frequency of the vessel roll motion.

Fig. 4 shows an upward-moving FS subjected to forces, where F_b is the buoyancy, $F_{gravity}$ is the gravity, F_{wave} is the wave excitations, $F_{inert.}$ is the inertial force, and F_d is the quadratic drag force. Among these components, F_d is the primary source of energy dissipation. It can be written as [8]

$$F_d(t)=-\frac{1}{2}\rho\cdot C_D\cdot A_{FS}\cdot u(t)\cdot|u(t)| \tag{3}$$

where ρ is the water density, C_D is the nondimensional drag coefficient, A_{FS} is the projected area in z direction, and u is the relative velocity between FS and water particle. u is approximated as the FS velocity here.

Then the energy dissipated by an FS during one cycle can be approximated by

$$E=\int_0^T F_d\,\mathrm{d}z_{FS}=\frac{4}{3}\rho\cdot C_D\cdot A_{FS}\cdot\eta_s^3\cdot\omega^2 \tag{4}$$

Alternatively, the equivalent linear damping coefficient in Eq.(1) during one cycle can be expressed as [6]

$$\overline{B_{44}}=\frac{E}{\pi\omega\cdot\phi_a^2} \tag{5}$$

Thus, given the FS properties and the vessel motion amplitude, the equivalent linear damping on the vessel can be estimated as

$$\overline{B_{44}}=\frac{4\rho\cdot C_D\cdot A_{FS}\cdot\eta_s^3\cdot\omega}{3\pi\cdot\phi_a^2} \tag{6}$$

Copyright © 2017 ASME

Downloaded From: http://proceedings.asmedigitalcollection.asme.org/ on 09/28/2017 Terms of Use: http://www.asme.org/about-asme/terms-of-use

Since η_s is almost proportional to ϕ_a, $\overline{B_{44}}$ linearly increases with the vessel roll amplitude ϕ_a. Eq.(6) implies that the FS and the vessel are rigidly connected, and the dissipated energy of FS is entirely absorbed by the vessel roll motion.

ANALYSIS PROCEDURE

Fig. 5 shows the procedure followed in this paper to assess the technical feasibility of an FS as a passive compensation device for the motions of the jack-up legs. In practice, the jack-up barges can be positioned with their best headings in view of motion responses. Therefore, the effectiveness of the proposed concept (jack-up barge with FS) should be assessed for a range of these headings of the barge. A fair comparison of the jack-up with or without FS can be done in terms of allowable limits of sea states.

Step 1 is to determine a suitable location of the FS for roll reduction of the barge. The initial position can be at midship, starboard or port side. Step 2 is to assess the location of the jack-up prone to the largest impact velocities. This can be done using global motion analysis for a jack-up barge without FS under different wave headings. In step 3, one determines the most favorable range of headings of a jack-up barge without FS. For this range of headings, a characteristic value of the impact velocity can be computed. This characteristic value will depend on the consequences of failure events and duration of the marine operation [5]. Steps 4 and 5 are to evaluate the characteristic values for the jack-up barge with and without FS, respectively. Steps 6 and 7 are to provide the operational limits in terms of allowable limits of sea states, by comparing the characteristic values with allowable limits of impact velocities. In step 8, one compares the H_s (T_p) limits of the jack-up barge with and without FS.

The analysis procedure given in this section is applied later to a case study, and the results and findings are given in detail in the section of Results and Discussions.

SYSTEM MODELING

System Components

The system consists of three bodies: a barge, a hook, and an FS. The barge and the hook are connected by a lift wire. The hook and the FS are connected by four sling wires, see Fig. 2. The main particulars are listed in Table 1, in which the vessel parameters refer to the condition before leg touchdown, and the origin of the coordinate system is placed at midship and at mean water level. The heave, roll, and pitch natural periods of the barge fall within the wave-frequency range. Because of the weight of the FS and relevant parts, the vessel payload can reduce by approximately 120 Ton.

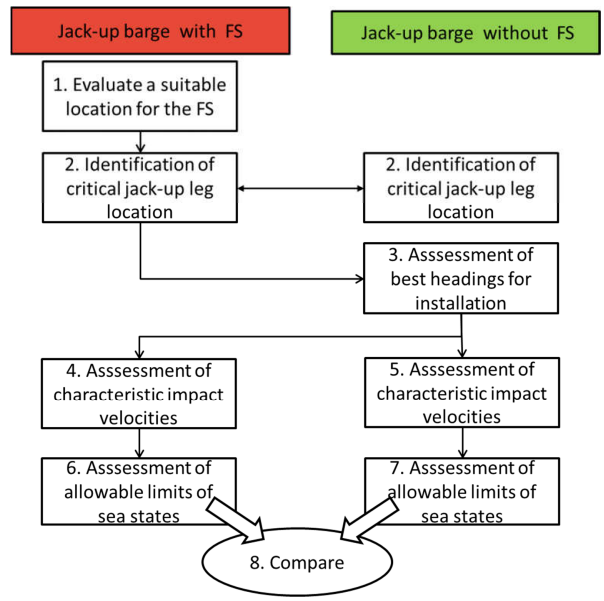

FIGURE 5. Analysis procedure

TABLE 1. Main particulars of the components

Parameter	*Symbol*	*Value*	*Units*
Jack-up barge			
Displacement	∇	6.81E4	Ton
Length overall	L_V	60	m
Breadth	B_V	33	m
Draught	T_V	3.6	m
Heave natural period	T_{n_3}	7.1	s
Roll natural period	T_{n_4}	7.5	s
Pitch natural period	T_{n_5}	8.2	s
Leg diameter	Dia_L	1.25	m
Leg length submerged	Len_L	29	m
Hook			
Mass	M_H	10	Ton
z-coordinate	z_H	-10	m
Flopper stopper			
Mass	M_{FS}	100	Ton
Length	L_{FS}	10	m
Breadth	L_{FS}	5	m
x-coordinate	x_{FS}	0	m
y-coordinate	y_{FS}	-21.6	m
z-coordinate	z_{FS}	-20	m
Lift wire			
Length	L_{LW}	15	m
Stiffness	K_{LW}	1.08E5	kN/m
Sling wire			
Length	L_{SW}	11.46	m
Stiffness	K_{SW}	1.75E5	kN/m

Copyright © 2017 ASME

Downloaded From: http://proceedings.asmedigitalcollection.asme.org/ on 09/28/2017 Terms of Use: http://www.asme.org/about-asme/terms-of-use

Coupled Dynamic Analysis

There are wire couplings between the barge and the hook, and between the hook and the FS. These coupling forces are tensile and modeled as linear springs. Connection flexibility is accounted for.

The equations of motion for the three-body system include 15 DOF's in total: six DOF for the barge and the FS each, and three translational DOF for the hook. The equations of motions are solved in the time domain by Newmark-Beta numerical integration with a time step of 0.001 s [9].

Hydrodynamic Forces on the Bodies

The first- and second-order hydrodynamic excitations on the barge are obtained using the potential theory [10]. The second-order loads in surge, sway, and yaw are calculated based on Newman's approximation and only the difference-frequency part is considered [11]. Due to the viscous loads on the barge and mooring lines, there exists damping for barge motions. These damping coefficients are represented as linear ones and selected according to [12]. The barge viscous damping in roll is estimated using the Ikeda formula for barges [13]. The linear damping coefficient is calculated as 1.52E+08 Nm/(rad/s) around the roll natural period.

The viscous effects on the legs and the FS can be important for wave-frequency motions. Each leg and spud can is treated as one slender element. The FS is represented by four equivalent slender elements circumferentially. According to Morison's formula for a moving cylinder [8], the hydrodynamic force per unit length normal to each strip can be determined as follows

$$f_s = \rho C_M \frac{\pi D^2}{4}\ddot{x}_w - \rho C_A \frac{\pi D^2}{4}\ddot{\eta}_1 + \frac{1}{2}\rho C_D D(\dot{x}_w - \dot{\eta}_1)|\dot{x}_w - \dot{\eta}_1| \tag{7}$$

where C_M, C_A, and C_D are the mass, added mass. and quadratic drag coefficients, respectively. $\dot{x}_w$ and $\ddot{x}_w$ are the velocity and acceleration of water particle at the strip center. $\dot{\eta}_1$ and $\ddot{\eta}_1$ are the velocity and acceleration of each strip. In the equation, the first term includes the Froude-Kriloff (FK) and diffraction force, the second term is the inertial force, and the last term the quadratic drag force [8].

The drag coefficients are dependent on *KC* number, Reynolds number, and surface roughness [14]. For complex structures like FS, experiments or computational fluid dynamics analysis are often involved to determine the coefficients accurately [15, 16, 17]. Here, a nondimensional C_D of 7.0 is selected based on experimental data on subsea structures [18]. For each slender element, the nondimensisonal C_A in heave is 7.45. It is calculated by WADAM [19]. For each leg cross section, a C_D of 0.9 is chosen according to [14].

CASE STUDY

Fig. 6 illustrates the coordinate system of the moored barge. The legs are symmetrical about the *x* and *y* axes, with a distance of 22.4 m from the midship and 13.8 m from the centreline. Table 2 lists the load cases considered. In this table, *LC* stands for load case, and *Dir* wave heading. Only one FS is placed on the starboard side in all simulations. Each simulation in *LC*1 lasts 500 sec. In *LC*'s 2-3, a white noise spectrum with a constant energy density of 0.05 m^2s/rad is applied, and each simulation lasts 3600 sec. In practice, the jack-up leg lowering process from a spud can of a few meters above seabed may last approximately 30 minutes. Thus, each simulation in *LC*'s 4-6 lasts 1800 sec. For each combination of H_s, T_p, and *Dir*, six simulations are run using different seed numbers. Long-crested waves are generated using the JONSWAP spectrum [20]. The aforementioned simulation length of the dynamic analysis refers to the length without start-up transients.

TABLE 2. Load cases

LC	H_s [m]	T_p [s]	*Dir* [deg]	*Notes*
1	/	/	90, 270	Regular, barge & FS
2	/	/	90, 135, 170	White noise (H_s=1.2 m), barge
3	/	/	90, 135, 170	White noise (H_s=1.2 m), barge & FS
4	0.2, 0.4, ... 1.6	5, 6, ...10	90, 135, 170	Irregular, barge
5	0.2, 0.4, ... 1.6	5, 6, ...10	90, 135, 170	Irregular, barge & FS

RESULTS AND DISCUSSIONS

Global Motion Characteristics

Figs. 7–10 show the cyclic variation of selected barge or FS responses over two wave periods. There can be significant differences in the barge roll amplitude depending on the side of deployment of the FS. As shown in Fig. 7(a), the maximum roll amplitude is 6 deg when the FS is positioned on the weather side, but the amplitude increases to 8.5 deg in Fig. 9(a). This difference is due to the roll-heave coupling, as noted in [7]. When the FS is deployed on the 'weather-side' (*Dir*=90 deg), the heave and roll velocities are mostly out of phase (Fig. 7(b)), causing the FS to move upwards with a velocity due to roll acting in conjunction with the upward velocity of heave. Hence, the FS velocity, hydrodynamic force, and damping moment are increased (Figs. 7(c)– 8(b). In contrast, when the FS is deployed on the 'lee-side' (*Dir*=270 deg), the heave and roll velocities are more in phase (Fig. 9(b)), causing a reduction in the FS velocity and damping effects, see Figs. 9(c)– 10(b)). The hydrodynamic forces on the FS are shown in Fig. 8(a) and Fig. 10(a), respectively. Among the components, the quadratic

Copyright © 2017 ASME

Downloaded From: http://proceedings.asmedigitalcollection.asme.org/ on 09/28/2017 Terms of Use: http://www.asme.org/about-asme/terms-of-use

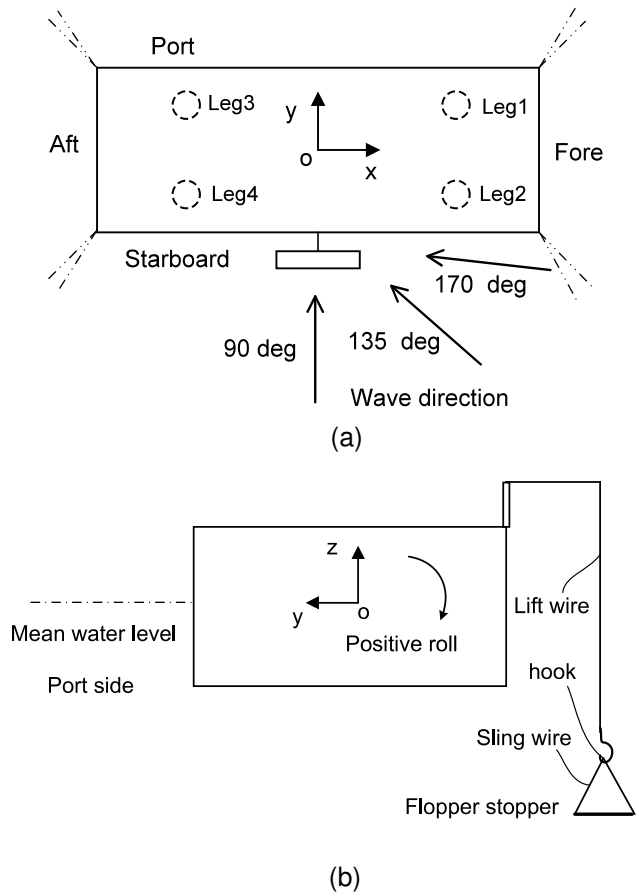

FIGURE 6. Vessel coordinate system (a) Top view (b) Aft view

drag dominates, but the inertial term may affect the form of the total force. The inertial term is due to the added mass and vertical acceleration of the FS. The FK and diffraction term has a minor impact on the total force. The dynamic coupling force is acting on the winch point at starboard. A correlation between the hydrodynamic and coupling forces can be observed. Like the roll motion, the resultant moment is positive clockwise. Equation 8 is used to quantify the instantaneous damping effect on the barge:

$$B_{44,FS}(t) = \frac{-M_C(t)}{\ddot{\phi}(t)} = \frac{-F_C(t) \cdot y_{FS}}{\ddot{\phi}(t)} \tag{8}$$

where $B_{44,FS}$ is the linear damping, F_C is the dynamic coupling force on the barge, and M_C is the moment from the coupling force.

As indicated by Figs. 8(c) and 10(c), the time-averaged linear damping varies appreciably. In the former case, negative damping occurs less than 10% of the time; in the latter, negative damping occurs more than 30% of the time and undermines the positive effect of FS.

Fig. 11 shows the computed average linear roll damping from FS for a number of roll amplitudes. When calculating the dissipated energy E, Eq.(5) uses the drag forces output from simulations, and verifies the simplified equation (6) despite a disparity for roll amplitudes above 7 deg. Compared with the more accurate expression Eq.(8), Eq.(6) overestimates the linear damping, especially at larger roll amplitudes; the discrepancy is 30% on average. The barge viscous damping and radiation damping are references in the dimensioning of FS. As shown, the current design of FS (10 by 5 m) only provides larger damping than the radiation damping when the roll motion exceeds 6 deg. For a more effective FS at lower sea states, a larger FS may be required. For Dir=270 deg, the damping due to FS is almost an order less and not presented here.

The impact forces on the legs of jack-up barges are of concern. Based on the conservation of energy for the worst-case scenario, the rotational energy of the barge is absorbed by the legs and support structures during the impact [21]. We focus on the total velocity of at leg tip, which is the sum vector of translational velocities:

$$V_{tot} = \sqrt{V_x^2 + V_y^2 + V_z^2} \tag{9}$$

where V_x, V_y and V_z are the velocities in surge, sway, and heave, respectively. Because the legs have large submerged length, V_x is mainly due to pitch, and V_y roll.

The legs on the 'weather-side' have larger motions. Leg2 in Fig. 6(a) is selected in the following analysis. The response amplitude operator (RAO) of the leg-tip velocities are examined here. Given input and output spectra, the RAO magnitude of a linear system can be expressed as

$$|H(\omega)| = \sqrt{\frac{S_{yy}(\omega)}{S_{xx}(\omega)}} \tag{10}$$

where S_{xx} denotes the input spectral density of the white noise of wave elevation, and S_{yy} the interested velocity spectrum.

As shown in Fig. 12(a), when the FS is deployed at starboard, the RAO of the total velocity is lower than that under a barge-alone condition for 90-deg wave heading. However, when the wave heading increases to 135 deg, the use of FS does not necessarily reduce the RAO for certain periods, see Fig. 12(b). This observation can be explained by the component

Copyright © 2017 ASME

Downloaded From: http://proceedings.asmedigitalcollection.asme.org/ on 09/28/2017 Terms of Use: http://www.asme.org/about-asme/terms-of-use

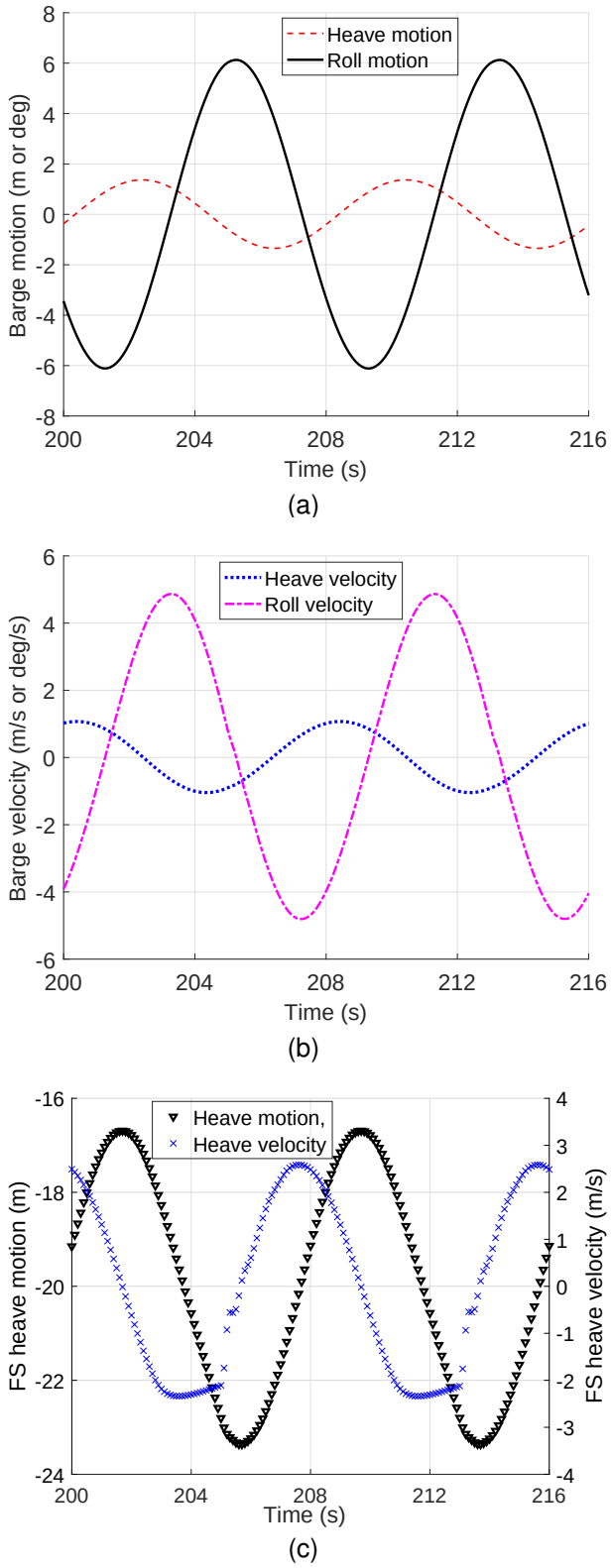

FIGURE 7. Time series of selected motion responses in regular waves ($LC1$, Dir=90 deg, H=1.4 m, T=8 s)

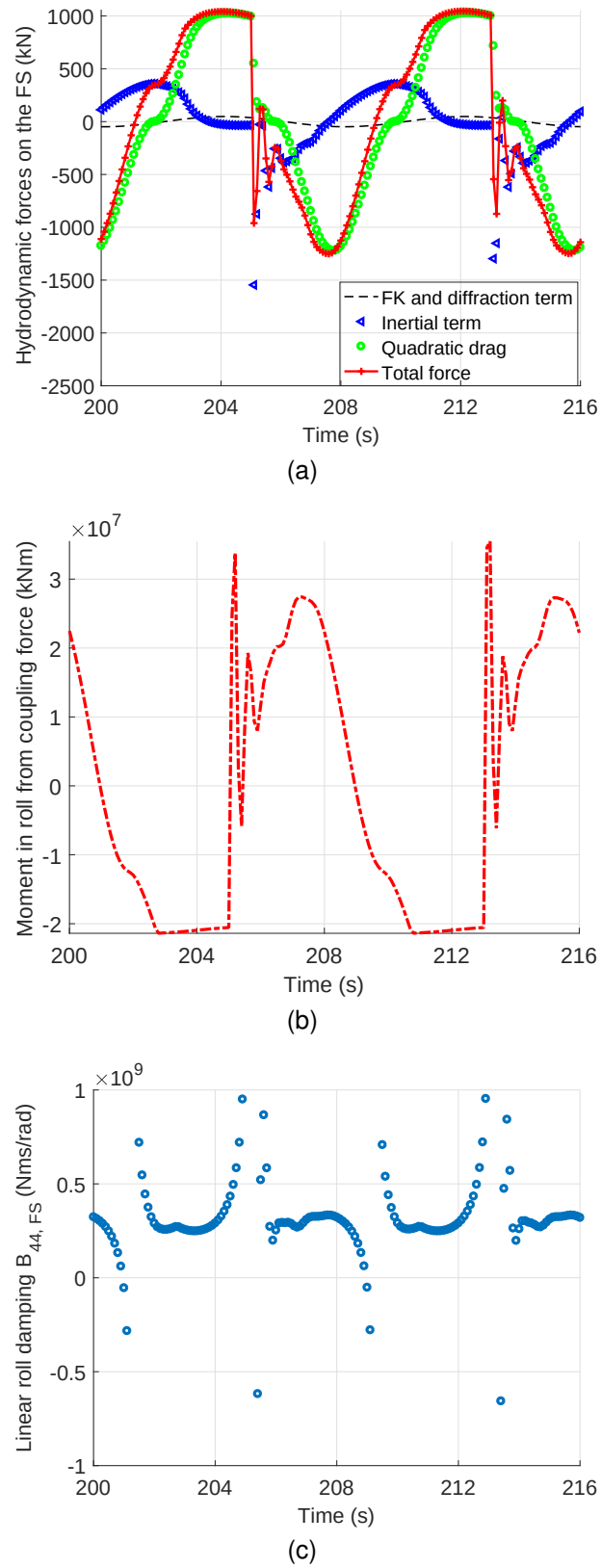

FIGURE 8. Time series of selected response variables in regular waves ($LC1$, Dir=90 deg, H=1.4 m, T=8 s)

Copyright © 2017 ASME

Downloaded From: http://proceedings.asmedigitalcollection.asme.org/ on 09/28/2017 Terms of Use: http://www.asme.org/about-asme/terms-of-use

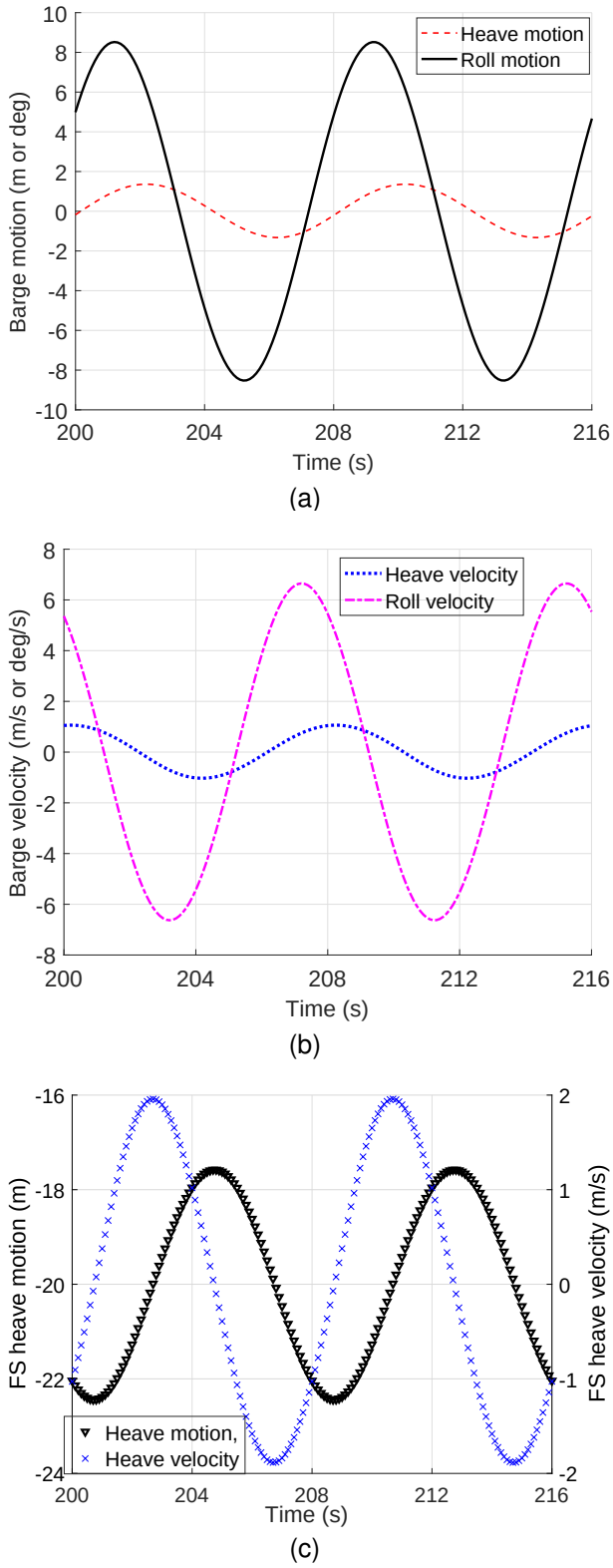

FIGURE 9. Time series of selected motion responses in regular waves (*LC*1, *Dir*=270 deg, *H*=1.4 m, *T*=8 s)

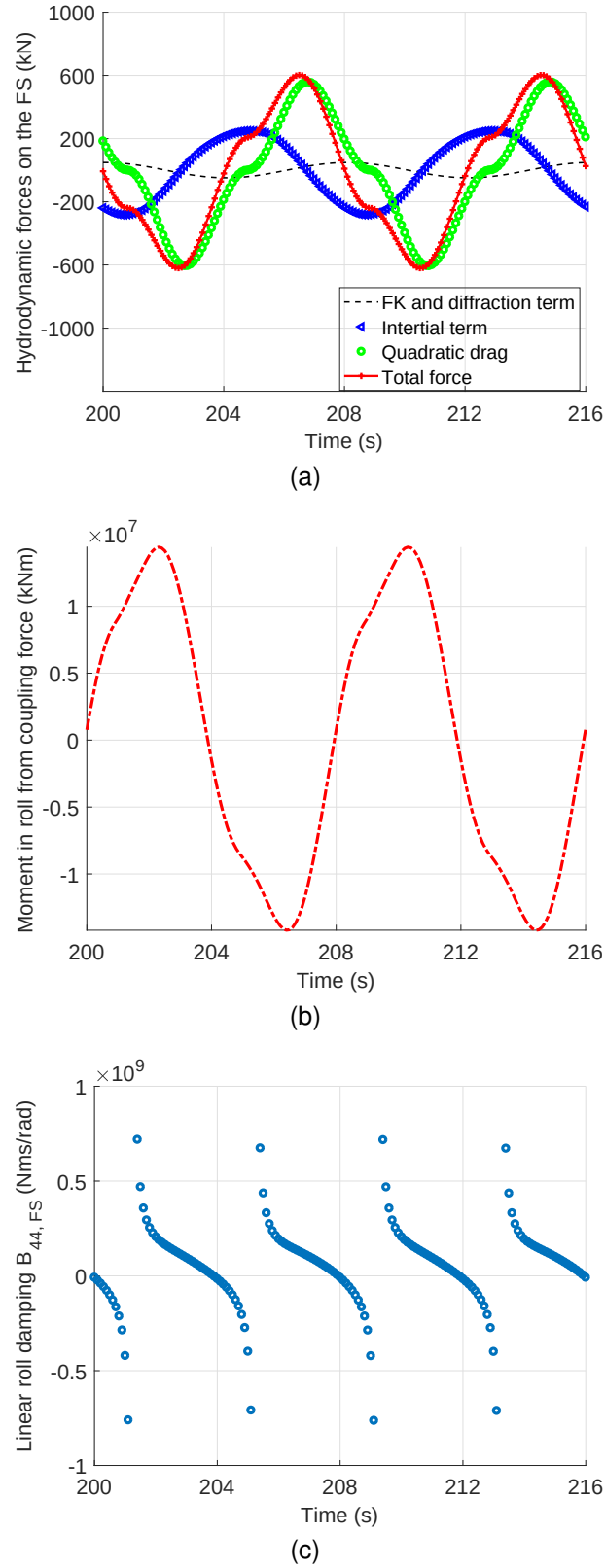

FIGURE 10. Time series of selected response variables in regular waves (*LC*1, *Dir*=270 deg, *H*=1.4 m, *T*=8 s)

Copyright © 2017 ASME

Downloaded From: http://proceedings.asmedigitalcollection.asme.org/ on 09/28/2017 Terms of Use: http://www.asme.org/about-asme/terms-of-use

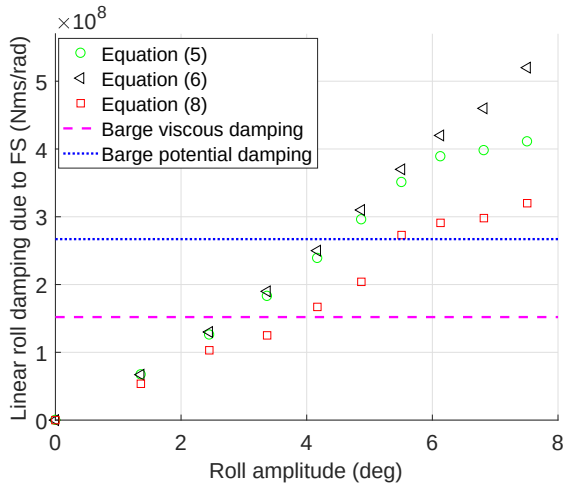

FIGURE 11. Variation of linear roll damping with roll amplitude, $LC1$, Dir=90 deg, T=8 s

RAO's plotted in Figs. 13– 15. For the 90-deg wave heading, V_x is negligible, but V_y is dominant. A significant reduction in V_y is found in Fig. 14(a) for the case with FS. This reduction is primarily attributable to the roll RAO of the vessel, see Fig. 16(a). The heave and pitch RAO's are less influenced by the FS and thus not presented. When the wave heading turns to 135 deg, the FS is still effective in reducing roll motion for most of the wave periods between 6 and 10 sec (Fig. 16(b)), but V_x is playing a more important role among the velocity components. V_x is associated with the pitch RAO, which is not affected. Accordingly, the impact of reduced V_y on the total velocity is minimal. For the 170-deg wave heading, the influence of V_x further increases, and the effect of FS aggravates.

Allowable Limits of Sea States

It is useful to know the allowable sea states for practical operations. For each 1800-sec simulation among LC's 4–6, the maximum leg velocity is obtained, and the expected maximum, an average of six global maxima, is used as a characteristic value. The allowable limit of the impact velocity of the leg should be determined by a leg-soil impact analysis [22]. In this paper, this velocity is not derived but reasonably estimated based on information available [4]. For a specific allowable limit of the impact velocity and its corresponding characteristic value, a backward derivation of the corresponding H_s (T_p) limit is possible [5].

Fig. 17 presents the operational limits in terms of allowable limits of sea states for an allowable impact velocity of 1.6 m/s. In both figures, the maximum H_s is limited to 1.6 m. Regardless of the wave heading and load cases, the curves reach a valley near T_p=8 sec, which is close to the natural periods of roll and pitch.

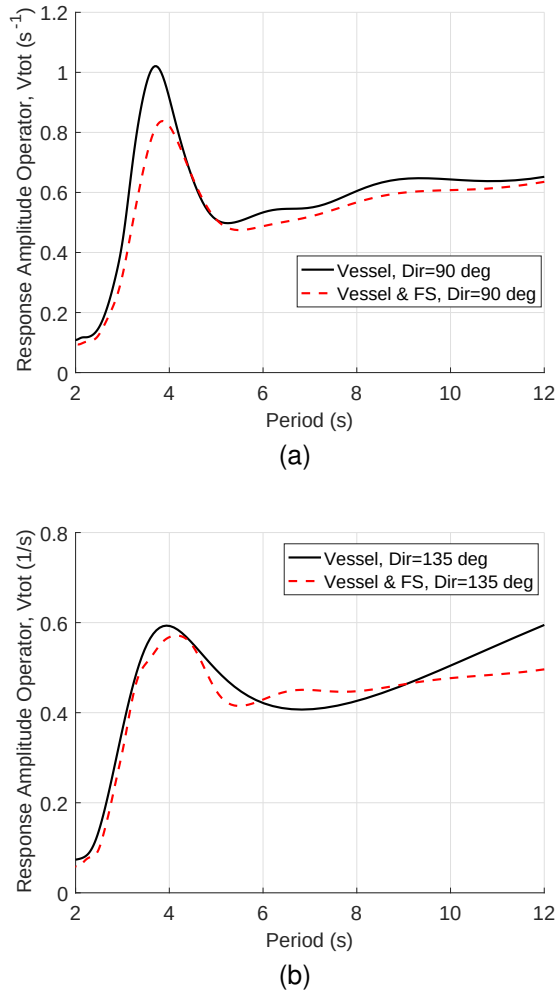

FIGURE 12. Comparison of RAO magnitude of the Leg2 tip, total velocity, $LC2$, 3 (a) Dir=90 deg (b) Dir=135 deg

For a fixed wave period, the limiting H_s (LH) is lowest at 90-deg heading. For any sea state, beam seas is expected to give greater leg motions than head seas. To assess the influence of FS, the relative increase (RI) in LH is defined as follows

$$RI = \frac{LH_i - LH_j}{LH_j} \times 100\ \% \tag{11}$$

where LH_i and LH_j stand for the limiting H_s in load cases i and j, respectively.

Fig. 18 compares the allowable sea states with and without FS. As shown, RI is equal to 0 at T_p=5 sec, because of the above-mentioned limitation in the maximum H_s. When Dir=90 deg, the increase in RI can be close to 40% for low wave periods.

Copyright © 2017 ASME

Downloaded From: http://proceedings.asmedigitalcollection.asme.org/ on 09/28/2017 Terms of Use: http://www.asme.org/about-asme/terms-of-use

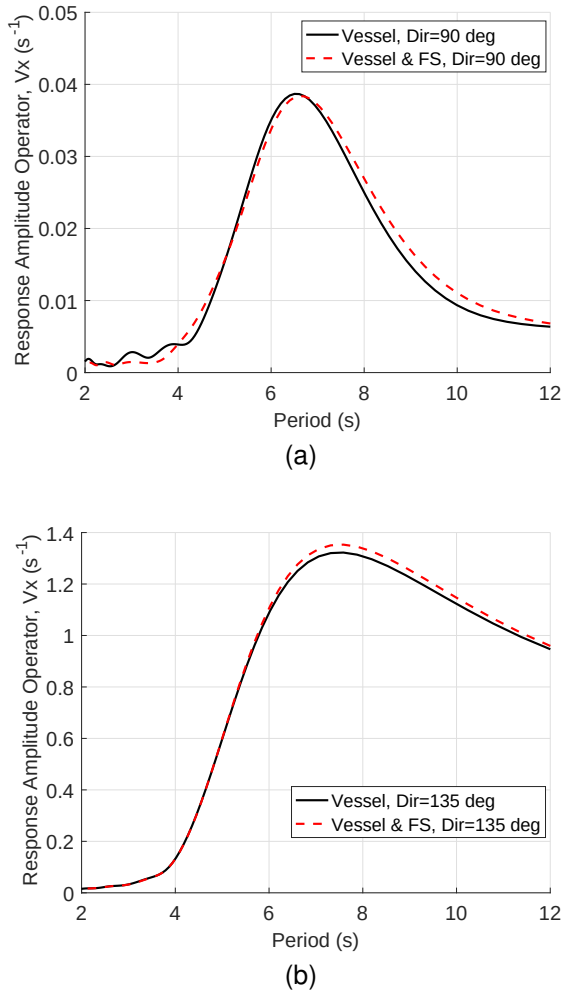

FIGURE 13. Comparison of RAO magnitude of the Leg2 tip, *x* velocity, *LC*2, 3 (a) *Dir*=90 deg (b) *Dir*=135 deg

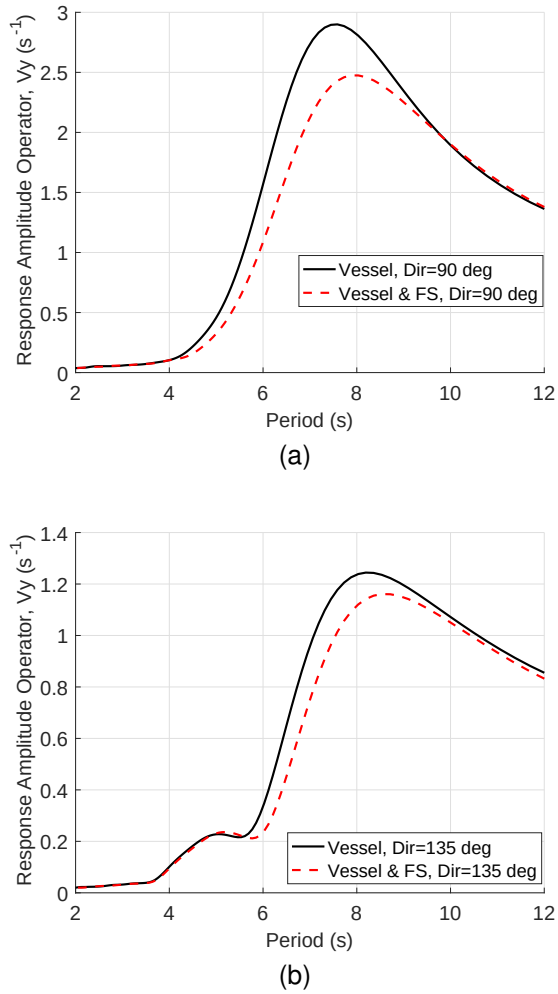

FIGURE 14. Comparison of RAO magnitude of the Leg2 tip, *y* velocity, *LC*2, 3 (a) *Dir*=90 deg (b) *Dir*=135 deg

The positive influence of the FS reduces for wave headings other than 90 deg. For 170-deg heading, *RI* can be close to -10% at higher T_p. This negative effect is related to the increase in the leg velocity RAO's.

The family of curves with typical allowable limits of impact velocities is shown in Fig. 19 for the beam seas condition. As shown, when an FS is used, the allowable limits of sea state is still sensitive to the impact velocity. For a specific barge, the allowable impact velocities should be established from finite element analysis.

CONCLUSIONS

This study explores the potential of flopper stoppers for application to jack-up barges. The flopper stopper is designed to be a template-like structures composed of plates and beams. We established a coupled system model with 15 degrees-of-freedom and performed numerical simulations in the time domain. The following conclusions are drawn:

1) If a single FS is used, the performance can vary significantly depending on its deployment position. For better damping effects, the FS should be deployed from the 'weather-side'of the vessel. For offshore wind turbine maintenance and repair, cranes are often placed on the 'weather-side', too. In practice, FS can be positioned towards the vessel bow to avoid collision. The deck arrangement is, nevertheless, not evaluated here.

2) The dimension of FS affects its effectiveness. Deploying an FS with a dimension of 10 by 5 m at starboard, the additional roll damping it provides is close to the original damping of the barge when the vessel roll nears 5 deg. When the leg-tip

Copyright © 2017 ASME

Downloaded From: http://proceedings.asmedigitalcollection.asme.org/ on 09/28/2017 Terms of Use: http://www.asme.org/about-asme/terms-of-use

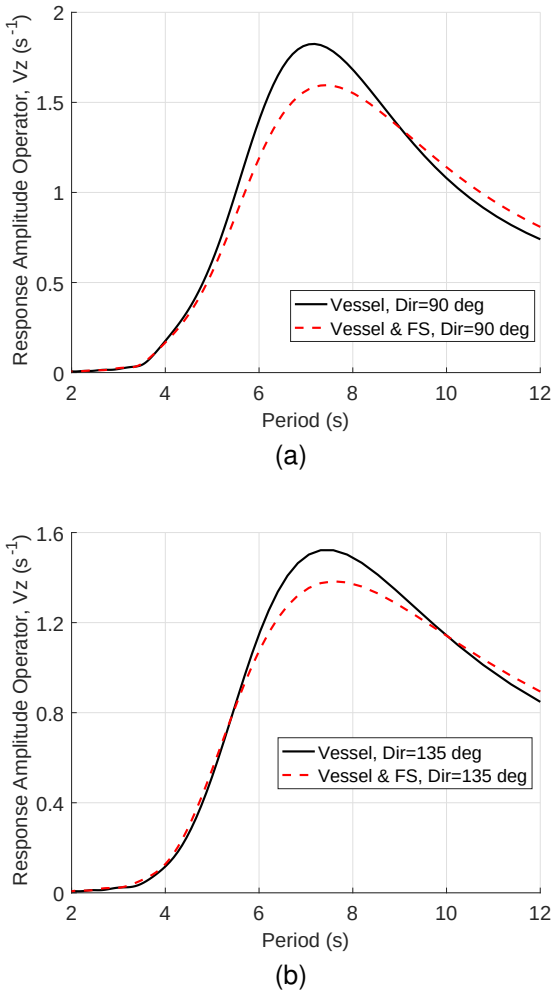

FIGURE 15. Comparison of RAO magnitude of the Leg2 tip, z velocity, $LC2$, 3 (a) Dir=90 deg (b) Dir=135 deg

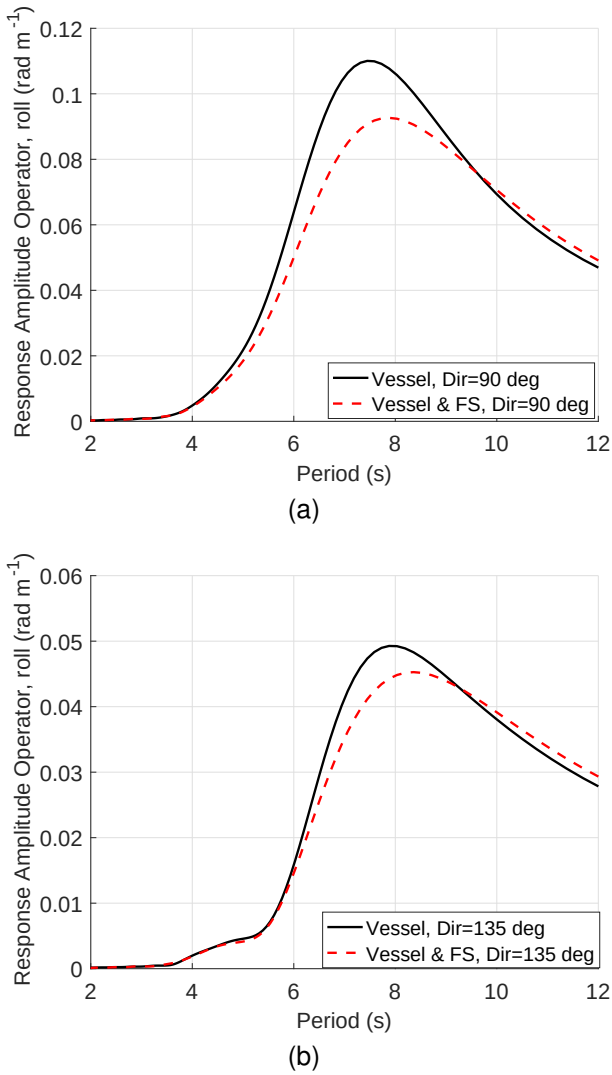

FIGURE 16. Comparison of RAO magnitude of the barge roll motion, $LC2$, 3 (a) Dir=90 deg (b) Dir=135 deg

velocities are concerned, the FS reduces the velocity responses in sway and heave directions, but not necessarily in the surge direction. Consequently, for 90-deg wave heading, the use of FS causes a maximum increase in the allowable wave height of 35%, but the effect can be much less or even negative for 135- or 170-deg headings.

3) The risk of collision between FS, wires, and vessel should be evaluated. In the irregular wave cases investigated, the minimum horizontal clearance between the FS and legs is greater than 2 meters, and the minimum horizontal clearance between the lift wire and the barge keel is greater than 3 meters. To reduce the risks of collision during lowering of the FS, it is recommended to lower the FS in head seas and to adjust the vessel heading afterwards.

4) For a better evaluation of the feasibility of FS, one needs to analyze a series of jack-up barges with varying properties. A design optimization of the FS should also be carried out. It is expected that for small vessels with limited damping from other sources, the effect of FS can be greater.

ACKNOWLEDGMENT

This work has been financially supported by the Research Council of Norway granted through the Department of Marine Technology and the Centre for Research-based innovation on Marine Operations from the Norwegian University of Science and Technology (NTNU). The first author thanks Peter Sandvik of MARINTEK and Yuna Zhao of NTNU for valuable discussions.

Copyright © 2017 ASME

Downloaded From: http://proceedings.asmedigitalcollection.asme.org/ on 09/28/2017 Terms of Use: http://www.asme.org/about-asme/terms-of-use

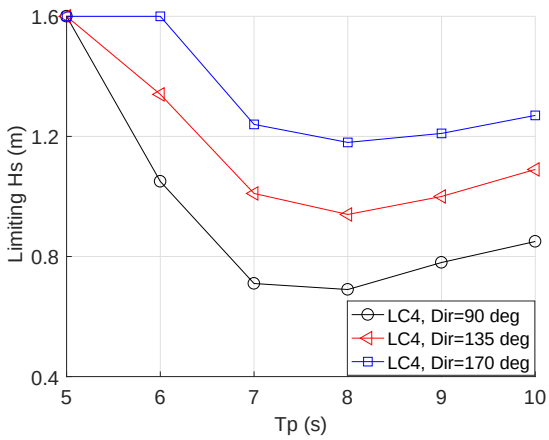

(a)

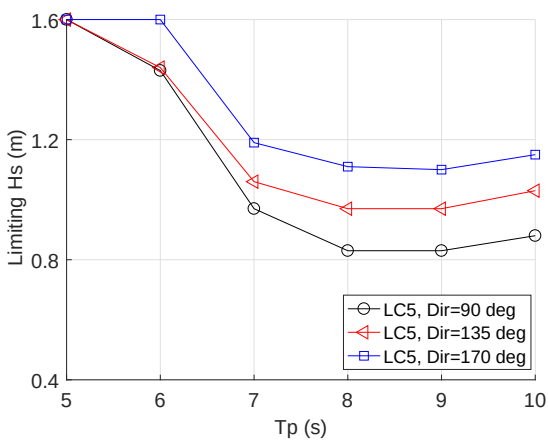

(b)

FIGURE 17. Allowable limits of sea states (V_{tot}=1.6 m/s, leg2) a) *LC*4, Barge alone (b) *LC*5, Barge & FS

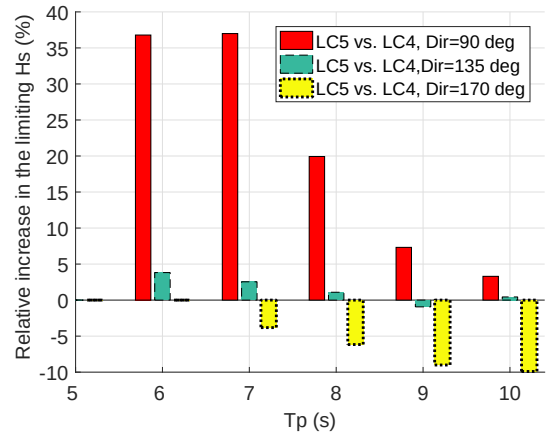

FIGURE 18. Percentage increase in the limiting wave heights (V_{tot}=1.6 m/s, leg2), *LC*5 (barge & FS) relative to *LC*4 (barge alone)

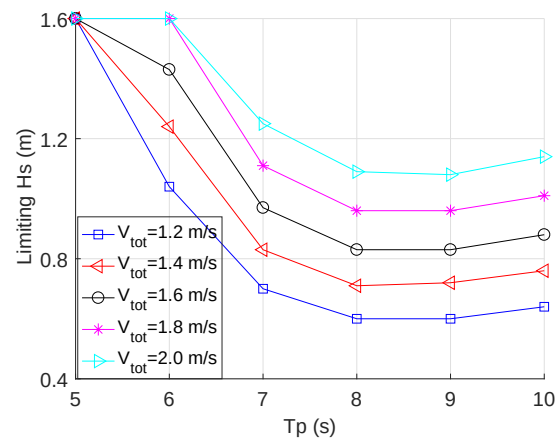

FIGURE 19. Effect of the limiting impact velocity on the allowable limits of sea state, leg2, *LC*5, *Dir*=90 deg

REFERENCES

[1] SetSail FPB, 2016 http://www.setsail.com/how-the-flopper-stoppers-work/. Accessed online on Dec. 16, 2016.

[2] Shenton, S., Mallet, C., and Frampton, M., 2014. Jack-up Vessel Optimisation: Improving Offshore Wind Performance through Better Use of Jack-up Vessels in the Operations and Maintenance Phase. The Crown Estate, 16 New Burlington Place, London, UK.

[3] Augener, P., and Hatecke, H., 2014. "Sea-keeping Analysis of an Offshore Wind Farm Installation Vessel during the Jack-up Process". In Proceedings of the ASME 33rd International Conference on Ocean, Offshore and Arctic Engineering, OMAE2014, San Francisco, USA.

[4] Smith, I., Lewis, T., Miller, B., and Lai, P., 1996. "Limiting Motions for Jack-Ups Moving onto Location". *Marine Structures,* ***9***, pp. 25–51.

[5] Guachamin Acero, W., Li, L., Gao, Z., and Moan, T., 2016. "Methodology for Assessment of the Operational Limits and Operability of Marine Operations". *Ocean Engineering,* ***125***, pp. 308–327.

[6] McCreight, W., and Jones, H., 1978. Prediction of the Effectiveness of Flopper-stopper Roll Damping Device. Technical Report, David W Taylor Naval Ship Research and Development Center Bethesda MD Ship Performance Department, USA.

[7] Bass, D., 1998. "Roll Stabilization for Small Fishing Vessels Using Paravanes and Anti-roll Tanks". *Marine Technology and SNAME News,* ***35***(2), pp. 74–84.

[8] Faltinsen, O.M., 1990. *Sea Loads on Ships and Offshore Structures*. Cambridge University Press, Cambridge, UK.

Copyright © 2017 ASME

Downloaded From: http://proceedings.asmedigitalcollection.asme.org/ on 09/28/2017 Terms of Use: http://www.asme.org/about-asme/terms-of-use

[9] MARINTEK, 2016. SIMO - Theory Manual Version 4.8.4.
[10] Lee, C., 1995. WAMIT Theory Manual. Department of Ocean Engineering, Massachusetts Institute of Technology, USA.
[11] Newman, J., 1974. "Second-order Slowly-varying Forces on Vessels in Irregular Waves". In International Symposium on the Dynamics of Marine Vehicles and Structures in Waves.
[12] Det Norske Veritas, 2013. Position Mooring, Offshore Standard, DNV-OS-E301.
[13] Ikeda, Y., Fujiwara, T., and Katayama, T., 1993. "Roll Damping of a Sharp Cornered Barge and Roll Control by a New-type Stabilizer". In Proceedings of the 3rd International Society of Offshore and Polar Engineers Conference, Vol.3, pp.634-639, Singapore.
[14] Det Norske Veritas, 2011. Modelling and Analysis of Marine Operations, Recommended Practice, DNV-RP-H103.
[15] Bunnik, T., Magee, A., and Buchner, B., 2004. "Experimental Investigation of Subsea Structures during Installation and the Related Wave Loads, Added Mass and Damping". In Proceedings of the 14th International Society of Offshore and Polar Engineers Conference, ISOPE-I-04-068, Toulon, France.
[16] Atluri, S., Magee, A., and K., L., 2009. "CFD as a Design Tool for Hydrodynamic Loading on Offshore Structures". In Proceedings of the ASME 28th International Conference on Ocean, Offshore and Arctic Engineering, OMAE2009, Honolulu, Hawaii, USA
[17] Sandvik, P., Solaas, F., and Firoozkoohi, R., 2016. "Hydrodynamic Forces on Complex Subsea Structures". In Marine Operations Special Symposium (MOSS 2016), Singapore.
[18] Øritsland, O., 1989. A Summary of Subsea Module Hydrodynamic Data, Marine Operations Part III.2. Technical Report, MARINTEK, Trondheim, Norway.
[19] Det Norske Veritas, 2010. WADAM user manual. Høvik, Norway.
[20] Hasselmann, K., Barnett, T., and Bouws, E. et al., 1973. Measurements of wind-wave growth and swell decay during the joint north sea wave project (JONSWAP), Technical Report, Deutches Hydrographisches Institut.
[21] Det Norske Veritas, 2012. Self-elvating Units, Recommended Practice, DNV-RP-C104.
[22] Ringsberg, J., Daun, V., and Olsson, F., 2015. "Analysis of Impact Loads on a Self-elevating Unit during Jacking Operation". In Proceedings of the ASME 34th International Conference on Ocean, Offshore and Arctic Engineering, OMAE2014, St. John's, Newfoundland, Canada.

Copyright © 2017 ASME

Downloaded From: http://proceedings.asmedigitalcollection.asme.org/ on 09/28/2017 Terms of Use: http://www.asme.org/about-asme/terms-of-use